WNK4 kinase is a physiological intracellular chloride sensor

Jen-Chi Chen[a,b], Yi-Fen Lo[a], Ya-Wen Lin[b], Shih-Hua Lin[a], Chou-Long Huang[c], and Chih-Jen Cheng[a,1]

[a]Division of Nephrology, Department of Medicine, Tri-Service General Hospital, National Defense Medical Center, Taipei 114, Taiwan; [b]Graduate Institute of Microbiology and Immunology, National Defense Medical Center, Taipei 114, Taiwan; and [c]Division of Nephrology, Department of Medicine, University of Iowa Carver College of Medicine, Iowa City, IA 52242-1081

Edited by Melanie H. Cobb, University of Texas Southwestern Medical Center, Dallas, TX, and approved January 11, 2019 (received for review October 7, 2018)

With-no-lysine (WNK) kinases regulate renal sodium-chloride cotransporter (NCC) to maintain body sodium and potassium homeostasis. Gain-of-function mutations of WNK1 and WNK4 in humans lead to a Mendelian hypertensive and hyperkalemic disease pseudohypoaldosteronism type II (PHAII). X-ray crystal structure and in vitro studies reveal chloride ion (Cl^-) binds to a hydrophobic pocket within the kinase domain of WNKs to inhibit its activity. The mechanism is thought to be important for physiological regulation of NCC by extracellular potassium. To test the hypothesis that WNK4 senses the intracellular concentration of Cl^- physiologically, we generated knockin mice carrying Cl^--insensitive mutant WNK4. These mice displayed hypertension, hyperkalemia, hyperactive NCC, and other features fully recapitulating human and mouse models of PHAII caused by gain-of-function WNK4. Lowering plasma potassium levels by dietary potassium restriction increased NCC activity in wild-type, but not in knockin, mice. NCC activity in knockin mice can be further enhanced by the administration of norepinephrine, a known activator of NCC. Raising plasma potassium by oral gavage of potassium inactivated NCC within 1 hour in wild-type mice, but had no effect in knockin mice. The results provide compelling support for the notion that WNK4 is a bona fide physiological intracellular Cl^- sensor and that Cl^- regulation of WNK4 underlies the mechanism of regulation of NCC by extracellular potassium.

chloride-sensing | potassium | pseudohypoaldosteronism type II | sodium chloride cotransporter | with-no-lysine kinase 4

With-no-lysine kinases (WNKs), a group of serine-threonine kinases with an atypical placement of the catalytic lysine, exert broad effects including cell volume control, transepithelial ion transport, and organ development (1). WNKs regulate SLC12 family cotransporters through downstream kinases Ste20-related proline/alanine-rich kinase (SPAK)/oxidative-stress response kinase-1 (OSR1) (2). Activated SPAK and OSR1 phosphorylate and activate the SLC12 cotransporters, such as Na^+-Cl^- cotransporter (NCC) and Na^+-K^+-$2Cl^-$ cotransporter (NKCC) (2). Gain-of-function mutations in *WNK1* and *WNK4* genes in humans cause a hypertensive and hyperkalemic disease known as pseudohypoaldosteronism type II (PHAII) (3).

Many advances have been made in our understanding of the regulation of WNKs (4). The discovery of Cullin3 and Kelch-like 3 (KLHL3) mutations in patients with PHAII without WNK1 or WNK4 mutations has led to better understanding of ubiquitin/proteasome-mediated proteolysis of WNKs (5–7). The recent crystallographic study of WNK1 kinase domain identifies a conserved Cl^--binding pocket near the catalytic site of the kinase domain, revealing a new regulatory pathway for the kinase activity of WNKs (8). The Cl^--bound WNK1 is prohibited from autophosphorylation and activation in the in vitro kinase assay. Replacing two critical leucines with phenylalanine disrupts the Cl^- binding and renders WNKs constitutively active (8–10). The effect on WNKs by intracellular Cl^- has been applied to explain how osmotic stress alters the catalytic activity of WNKs (11, 12). However, whether this actually occurs in vivo in actively transporting epithelia such as distal convoluted tubule (DCT) is unclear. In transporting epithelia, changes in concentrations of ions from exit across one membrane (e.g., basolateral) will be coupled by parallel entry on the other membrane (e.g., apical). The tight coupling between apical and basolateral transport to minimize fluctuations of intracellular concentration of solutes and cell volume is a fundamental homeostatic feature of transporting epithelia. Whether the intracellular concentration of Cl^- ($[Cl^-]_i$) in DCT under physiological conditions is within the dynamic range for modulating the activity of WNKs is unknown.

Unlike WNK1, which is widely expressed, WNK4 is expressed highly in the kidney, particularly in the NCC-expressing DCT (13). The function of WNK4 on NCC has been extensively investigated for almost 2 decades. An early study showed that WNK4-overexpressing transgenic mice exhibited hypotension and decreased NCC, suggesting the inhibitory role of WNK4 on NCC (14). In contrast, PHAII-mimicking WNK4 knockin mouse and another model of WNK4 transgenic mouse displayed hypertension and increased NCC, indicating the stimulatory effect of WNK4 on NCC (15). More recently, three independent studies reported that WNK4 knockout mice display Gitelman's syndrome with a drastically decreased NCC abundance and activity, supporting the notion that WNK4 is essential for NCC activity (16–18).

Transcellular movement of Cl^- plays an important role in fluid and electrolyte secretion and absorption in many epithelia (19). Work in shark rectal gland tubules has led to the hypothesis of the existence of intracellular Cl^- sensors activating unidentified kinases/phosphatases (11). In the kidney, dietary potassium (K^+) deprivation activates NCC, whereas K^+ loading turns off NCC (20, 21). These effects on NCC are believed to be important for

Significance

The existence of intracellular Cl^- sensors has long been postulated and sought after. Recent structural and in vitro results support that with-no-lysine (WNK) kinases, particularly WNK4, may function as Cl^- sensors. Here, we demonstrate that knockin mice carrying Cl^--insensitive WNK4 mutant phenocopy Mendelian disease and a previous mouse model caused by gain-of-function mutations of WNK4. Furthermore, Cl^--insensitive WNK4 knockin mice lose the expected WNK4-mediated stimulation of sodium-chloride cotransporter caused by hypokalemia-induced decreases in the intracellular concentration of Cl^-. Thus, WNK4 is a bona fide physiological intracellular Cl^- sensor. The results shed light on the pathophysiology of hypertension in potassium deficiency.

Author contributions: J.-C.C. and C.-J.C. designed research; J.-C.C. and Y.-F.L. performed research; J.-C.C., Y.-F.L., C.-L.H., and C.-J.C. analyzed data; and J.-C.C., Y.-F.L., Y.-W.L., S.-H.L., C.-L.H., and C.-J.C. wrote the paper.

The authors declare no conflict of interest.

This article is a PNAS Direct Submission.

[1]To whom correspondence should be addressed. Email: laurence1234kimo@yahoo.com.tw.

This article contains supporting information online at www.pnas.org/lookup/suppl/doi:10.1073/pnas.1817220116/-/DCSupplemental.

Published online February 14, 2019.

maintaining K^+ homeostasis and in the pathogenesis of K^+ deficiency-induced hypertension (22). Mechanistically, recent in vitro and ex vivo studies lend support for the hypothesis that extracellular K^+ modulates $[Cl^-]_i$ to regulate the activity of NCC via WNKs-SPAK/OSR1 cascade (9, 10, 23, 24). In the present study, we generated knockin mice carrying Cl^--insensitive WNK4 to test the hypothesis that WNK4 functions as a physiological Cl^- sensor. We manipulated dietary K^+ intake as an experimental approach to alter $[Cl^-]_i$, and used the activity of NCC as a readout for WNK4 activity.

Results

L319F/L321F WNK4 Knockin Mice Recapitulate Pseudohypoaldosteronism Type II. The hydrophobic pocket in the kinase domain of WNKs is central to the $[Cl^-]_i$-mediated regulation. To investigate the role of Cl^--sensing by WNK4 in vivo, we created knockin mice carrying L319F/L321F double-mutant WNK4, using CRISPR/Cas9 technology (Fig. 1 *A*–*C*). Mutant WNK4 knockin mice were viable and born at expected Mendelian ratios with normal gross appearance and body weight. The abundance of WNK4 protein in knockin mice was similar to wild-type (WT) mice (Fig. 1 *D* and *E*), indicating that the mutations did not alter the expression or stability of WNK4.

Eight-week-old knockin mice and WT littermates were fed standard chow and placed in metabolic cages. Compared with WT mice, knockin mice had relatively higher blood pressure, with a similar urinary Na^+ excretion rate in the steady state (Table 1). The steady-state urinary K^+ excretion was also the same between the two groups, but plasma K^+ concentration was higher and the calculated fractional excretion of K^+ lower in knockin versus WT mice, indicating that tubular K^+ secretion is impaired in knockin mice. Blood pH was not significantly different, whereas knockin mice exhibited lower plasma bicarbonate and total CO_2 levels than WT mice. Plasma $[Cl^-]$ was elevated in knockin mice relative to WT mice. Thus, Cl^--insensitive WNK4 knockin mice recapitulate the phenotypes of human PHAII featuring hypertension, hyperkalemia, and hyperchloremic metabolic acidosis.

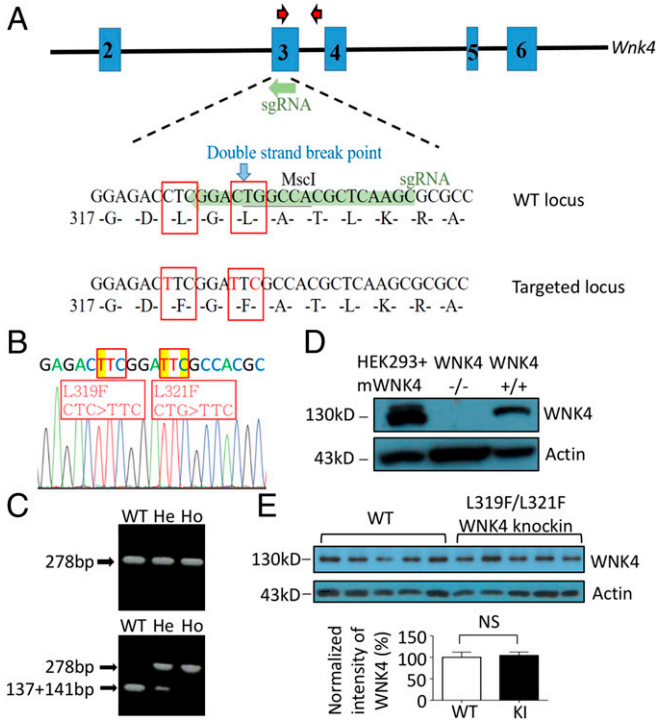

Fig. 1. Generation of L319F/L321F WNK4 knockin (KI) mice. (*A*) The sgRNA was designed to target a sequence spanning WNK4 amino acids 317–325 in exon 3 (WT locus highlighted in green). Cas9 induced a double-strand break at amino acid 321 (blue arrow), and donor DNA containing mutated L319F and L321F (targeted locus) was fused into WNK4 gene through homologous recombination. Red arrows marked the locations of primers used for genotyping. (*B*) Sequencing of WNK4 gene confirmed L319F and L321F mutations. (*C*) Genotyping of L319F/L321F WNK4 KI mice was carried out using PCR-based restriction analysis. The 278-bp products (*Upper*) were digested with MscI. MscI recognized 5′ TGGCCA 3′ and cut WT product into two fragments (137 and 141 bp; *Lower*). He, heterozygous; Ho, homozygous. (*D*) Verification of anti-mouse WNK4 antibody by Western blot analysis. Mouse WNK4 was detected in the lysate of HEK293 cells transfected with mouse WNK4 plasmids (HEK293+mWNK4) and whole-kidney lysate of WT ($WNK4^{+/+}$) mice, but not in WNK4 knockout ($WNK4^{-/-}$) mice. (*E*) Western blot analysis of WNK4 protein (*Upper* ~130 kDa) in whole-kidney lysates of WNK4 KI ($n = 5$) mice and their WT ($n = 5$) littermates. Actin (*Lower* ~42 kDa) was used as a loading control. The results were quantified by using ImageJ. NS, statistically not significant.

Activation of NCC and Inhibition of ENaC in Cl^--Insensitive WNK4 Knockin Mice. We further investigated the molecular mechanism of hypertension in knockin mice by examining the activity and protein abundance of NCC, NKCC2, and epithelial Na^+ channel (ENaC) in the distal nephron. Western blot analysis and immunofluorescence found that both total NCC and T58 phospho-NCC were significantly increased in knockin WNK4 mice (Fig. 2*A* and *SI Appendix*, Fig. S1). We used thiazide-sensitive urinary Na^+ excretion rate (ΔUNa; thiazide minus vehicle) as a readout for in vivo NCC activity. Knockin mice displayed a significantly higher thiazide-sensitive urinary Na^+ excretion rate than WT littermates (Fig. 2*E*; $P < 0.001$). Knockin mice and WT mice had a similar amount of total NKCC2 and S130 phospho-NKCC2 (Fig. 2*B* and *SI Appendix*, Fig. S2) and furosemide-sensitive urinary Na^+ excretion rate (Fig. 2*F*). Activation of ENaC requires proteolytic cleavage in the extracellular domains of α and γ subunits (25). We examined the full-length and cleaved forms of α and γENaC (Fig. 2*C*). Full-length and cleaved forms of αENaC were not significantly different between WT and knockin mice. However, the cleaved form of γENaC and the ratio of cleaved form versus full-length γENaC in knockin mice were notably reduced compared with WT controls. We also checked βENaC and found no difference between WT and knockin mice (*SI Appendix*, Fig. S3*A*). Amiloride-sensitive urinary Na^+ excretion rate was lower in knockin mice than WT controls, indicating decreased ENaC activity in knockin mice (Fig. 2*G*; $P = 0.027$). We examined the abundance of the total and phospho-SPAK/OSR1. There was no significant difference in the amount of total SPAK/OSR1 between knockin and WT mice, but the abundance of S373 and S233 phospho-SPAK/OSR1 was higher in knockin than WT mice (Fig. 2*D* and *SI Appendix*, Fig. S3*B*). The results are consistent with the notion that knockin mice have increased WNK4 activity, which leads to the activation of NCC via SPAK/OSR1 cascade. The expression and subcellular distribution of ROMK in collecting ducts of knockin mice were not significantly different from that of WT mice (*SI Appendix*, Figs. S3*C* and S4), suggesting that hyperactive NCC with reduced distal Na^+ delivery and decreased ENaC activity are the main causes of hyperkalemia in knockin mice.

Potassium Deprivation Enhances NCC Through Cl^--Sensing Regulation on WNK4. Low dietary K^+ intake has been linked to hypertension and activation of NCC in human cohorts and animal studies (26, 27). Recent studies suggest that hypokalemia from dietary K^+ restriction enhances basolateral Cl^- exit, resulting in falls in $[Cl^-]_i$ and activation of WNK4 and NCC (10, 23). We examined the effects of dietary K^+ restriction on NCC in knockin mice to further test the hypothesis that WNK4 functions as an intracellular Cl^- sensor and investigate the mechanism of NCC activation by K^+ deficiency. WT and knockin mice were fed control K^+ (1% K^+) or K^+-deficient (<0.03% K^+) diets. On K^+-deficient

Table 1. Plasma and urine biochemistries in Wnk4 L319F/L321F KI and WT mice

Group	WT (n = 12)	KI (n = 12)
Body weight, g	19.4 ± 1.0	19.9 ± 1.0
Blood pressure, mm Hg	105 ± 2.1/64 ± 1.6	114 ± 3.0*/71 ± 1.9*
Plasma		
BUN, mg/dL	26.5 ± 1.7	25.7 ± 1.6
Creatinine, mg/dL	0.25 ± 0.03	0.24 ± 0.03
Na^+, mM	151.5 ± 0.56	151.8 ± 0.68
K^+, mM	4.37 ± 0.10	4.75 ± 0.10*
Cl^-, mM	117.2 ± 0.75	119.3 ± 1.2*
Ca^{2+}, mg/dL	4.92 ± 0.11	4.95 ± 0.10
Mg^{2+}, mg/dL	2.87 ± 0.07	2.88 ± 0.08
Hb, g/dL	13.5 ± 0.16	13.7 ± 0.14
pH	7.36 ± 0.01	7.34 ± 0.01
HCO_3^-, mM	19.4 ± 0.51	17.6 ± 0.36*
Total CO_2, mM	20.1 ± 0.57	18.7 ± 0.38*
Urine		
Volume, mL	1.72 ± 0.21	1.52 ± 0.13
Na^+ excretion, μmol/h	6.1 ± 0.30	6.3 ± 0.17
K^+ excretion, μmol/h	11.2 ± 0.5	10.7 ± 0.3
FE_{Na}, %	0.34 ± 0.05	0.38 ± 0.03
FE_K, %	32.8 ± 1.4	26.8 ± 1.7*

FE, fractional excretion; KI, knockin. *P < 0.05.

diets, urinary K^+ excretion decreased to the trough level by 24–48 h (Fig. 3*A*). The rate of decrease was slightly but significantly slower in knockin versus WT mice, likely reflecting impaired tubular K^+ excretion and higher plasma K^+ levels at baseline in knockin mice. As reported before, plasma K^+ levels decreased after 4 d receiving K^+-deficient diets, although the levels remained higher in knockin mice than in WT mice (Fig. 3*C*; P = 0.0005). The calculated urinary fractional excretion of K^+ (reflecting tubular K^+ excretory ability) remained depressed in knockin versus WT mice.

For WT mice on K^+-deficient diets, urinary Na^+ excretion showed a gradual but consistent trend of decline, reaching ∼50% reduction by day 4 (Fig. 3*B*; P = 0.025). In contrast, Na^+ excretion in knockin mice remained relatively stable during the course. K^+ deprivation significantly increased thiazide-sensitive urinary Na^+ excretion rate in WT mice (P < 0.0001), but did not cause further increases beyond the already elevated levels in knockin mice (Fig. 3*D*). We next examined the abundance of NCC and ENaC in these mice. Consistent with the effects on thiazide-sensitive Na^+ excretion, K^+ deprivation significantly increased the abundance of total and phosphorylated NCC in WT mice, but did not cause further increases in knockin mice (Fig. 3*E*). Administration of norepinephrine, a known activator of NCC (28), significantly increased phosphorylated NCC in knockin mice (*SI Appendix*, Fig. S5), indicating that NCC in these mice remains responsive. Interestingly, dietary K^+ restriction significantly decreased the abundance of the cleaved γENaC in both WT and knockin mice. The dissociation between effects on NCC and ENaC suggests that down-regulation of ENaC is not simply a compensatory response to up-regulation of NCC. Overall, the above results support the notion that dietary K^+ restriction stimulates NCC and causes Na^+ retention. The fact that dietary K^+ restriction was not able to further increase NCC activity in Cl^--insensitive knockin mice indicates that Cl^- sensing by WNK4 is the underlying mechanism for up-regulation of NCC by dietary K^+ restriction.

Potassium Loading Inactivates NCC Despite Constitutively Active WNK4. Long-term K^+ loading inactivates NCC and stimulates ENaC and ROMK (20, 27). To determine whether the Cl^--sensing mechanism of WNK4 is involved in this process, we fed knockin mice and WT littermates control K^+ (1%) or high-K^+ (5%) diets for 4 d. Within 6 h of placing the mice on high-K^+ diets, urinary K^+ markedly increased in both groups (Fig. 4*A*). Compared with WT mice, knockin mice had higher urinary K^+ excretion rate in the first 0–24 h of the high-K^+ diet (P = 0.0008). The difference may be a result of transient relative hyperkalemia in knockin mice (Fig. 5*B*). Daily food intake was not different between two groups (*SI Appendix*, Fig. S6). However, small differences in intake within the first 6 h cannot be excluded. Urinary K^+ excretion remained up during days 2–4 of high-K^+ diets, and was not significantly different between knockin and WT mice. Consistent with the notion that K^+ loading causes natriuresis (29), urinary Na^+ excretion increased within 6 h of high-K^+ diets (Fig. 4*B*). Beyond the first 6 h, natriuresis partially subsided, but remained at the level higher than twofold of control K^+ diets. Diminished natriuretic response beyond the first 6 h may be partly a result of the activation of ENaC (21) and/or ensuing hypokalemia (vide infra).

To our initial surprise, hypokalemia developed on high-K^+ diets in both WT and knockin mice, although knockin mice still had a significantly higher plasma K^+ concentration than WT mice (Fig. 4*C*; P = 0.014). Further analyses reveal that this is likely because the magnitude of kaliuresis (∼2,400–3,600 μmol/d) far exceeds the intake (∼1,500 μmol/d; *SI Appendix*, Fig. S6). Sustained K^+ loading-induced natriuresis likely contributes to excessive kaliuresis, leading to K^+ wasting. We examined the activity and abundance of Na^+ transporters. By day 4 of high-K^+ diets, the thiazide-sensitive natriuresis was significantly reduced in

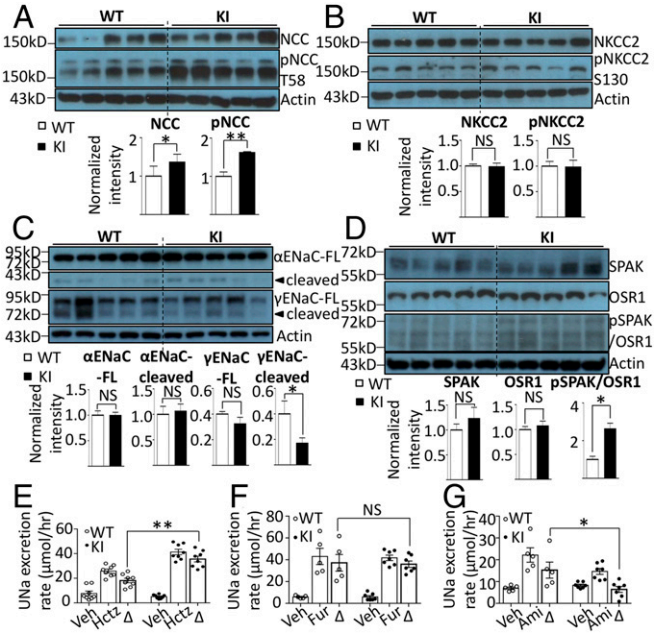

Fig. 2. Protein expression and activity of sodium transporters/channel and SPAK/OSR1 in L319F/L321F WNK4 KI mice. (*A–D*) Western blot analyses of (*A*) total NCC and T58 phospho-NCC, (*B*) total NKCC2 and S130 phospho-NKCC2, (*C*) full-length (FL) and cleaved forms of αENaC and γENaC, and (*D*) total SPAK, OSR1, and S373 phospho-SPAK/OSR1 in whole-kidney lysates of L319F/L321F WNK4 KI (n = 5) mice and their WT littermates (n = 5) in one experiment. Actin loading controls are shown for each blot. The protein expression was normalized to the amount of β-actin and reported relative to WT controls. The abundance of each band was measured by densitometry by the Image J program. (*E–G*) The effects of (*E*) hydrochlorothiazide (Hctz, 12.5 mg/kg), (*F*) furosemide (Fur, 15 mg/kg), or (*G*) Amiloride (Ami, 0.65 mg/kg) vs. vehicle (Veh) on the urinary Na^+ excretion rate were calculated. Diuretic-sensitive natriuresis (Δ) in WT and KI mice were compared. Results are presented as mean ± SEM, and data were analyzed by unpaired t test. *P < 0.05; **P < 0.01; NS, statistically not significant between indicated groups.

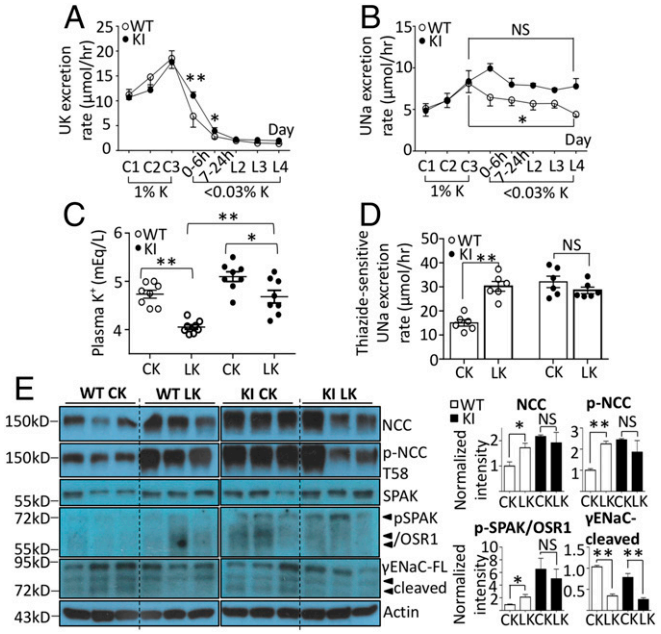

Fig. 3. Physiological and biochemical responses to K^+ deprivation in WNK4 KI and WT mice. WT and WNK4 KI mice were fed a control K^+ (CK; 1% K^+) diet for 3 d (C1–C3) and then a K^+-deficient diet (LK; <0.03% K^+) for 4 d (L1–L4). In the first day of LK, urine samples were collected twice in the first 6 h (0–6 h), and the rest in 18 h (7–24 h). (*A* and *B*) The urinary K^+ (UK) and Na^+ (UNa) excretion rates in WT and KI mice taking LK were compared. (*C*) The plasma K^+ levels of mice at the end of 4 d of CK or LK diet were measured. (*D*) By the end of K^+ deprivation, thiazide-sensitive UNa excretion rate in WT and KI mice taking CK or LK were compared. (*E*) The protein abundance of total NCC and T58 phospho-NCC, total SPAK and S373 phospho-SPAK/OSR1, and FL and cleaved forms of γENaC in whole-kidney lysates of WT and KI mice taking CK or LK diet ($n = 3$ for each group) were analyzed by Western blot. Arrowheads indicate the isoforms of phosphorylated SPAK/OSR1 and ENaC. Mice in the same experiment were compared. The result shown is the representative of at least three experiments with similar results. Each band was quantified by ImageJ. $^*P < 0.05$; $^{**}P < 0.01$; NS, statistically not significant between indicated groups using Student's *t* test.

both knockin and WT mice compared with control K^+ diets (Fig. 4*D*; $P < 0.0001$). Likewise, the abundance of total and phosphorylated NCC was reduced in knockin as well as WT mice (Fig. 4*E*). The fact that high-K^+ diets decrease NCC in knockin mice indicates that a mechanism other than Cl^- sensing by WNK4 is involved (*Discussion*). A high-K^+ diet markedly increased the abundance of cleaved γENaC in both WT and knockin mice.

Acute Potassium Loading Deactivates NCC Dependent on Cl^- Sensing of WNK4. Unexpected hypokalemia precludes us from using chronic K^+ loading to test the hypothesis that high extracellular K^+ inactivates NCC by increasing $[Cl^-]_i$ and inhibiting WNK4. We turned to acute K^+ loading by oral gavage, an approach that has been consistently shown to raise plasma $[K^+]$ and dephosphorylate NCC in 15–30 min (21). The abundance of phosphorylated NCC was markedly decreased in WT mice 30 min after oral gavage of K^+ (Fig. 5*A*). Supporting the hypothesis that Cl^- sensing by WNK4 is involved, K^+ gavage did not cause decreases in the abundance of phosphorylated NCC in knockin mice. The abundance of total NCC was not affected by K^+ gavage in both WT and knockin mice at 30 min. As reported before (21, 29), plasma K^+ levels rose acutely with oral K^+ gavage (Fig. 5*B*). Probably as a result of the underlying impairment in tubular K^+ excretion, plasma $[K^+]$ rose to a higher level in knockin mice than WT mice ($P = 0.024$). Unlike the effect on phosphorylated NCC, K^+ gavage increased the abundance of cleaved γENaC in both WT and knockin mice (Fig. 5*C*).

Discussion

Cl^- is the most abundant anion in the body fluid, and together with Na^+, it critically determines the extracellular volume status. That Cl^- also plays a signaling role has long been postulated, but is yet to be definitely proven. In the secretory epithelia of shark rectal glands, apical Cl^- exit stimulated by secretagogues is accompanied by phosphorylation of NKCC1 at the basolateral membrane, which is believed to mediate increases in Cl^- entry for transcellular movement (11). It was postulated that an intracellular sensor detects changes in $[Cl^-]_i$ leading to phosphorylation of NKCC1. The discovery by Piala et al. (8) that Cl^- binds and regulates WNK kinase activity opened the door for the hypothesis that WNKs are Cl^- sensors. To this support, studies have shown that in cultured cells, lowering extracellular K^+ hyperpolarizes cell membrane potentials, enhances cellular Cl^- exit, and leads to decreases in $[Cl^-]_i$ and increases in WNK kinase activity (10). Inverse correlation between extracellular $[K^+]$ and NCC phosphorylation in vivo (23) provide further support for the notion.

Direct evidence for the hypothesis, however, remains lacking. The function of transport epithelia is to move ions and fluid across with minimal perturbation of intracellular ionic concentrations and cell volume. In the setting of K^+ deficiency, decreases in $[Cl^-]_i$ in DCT under hypokalemia will increase the driving force for apical Cl^- entry through NCC. Depending on

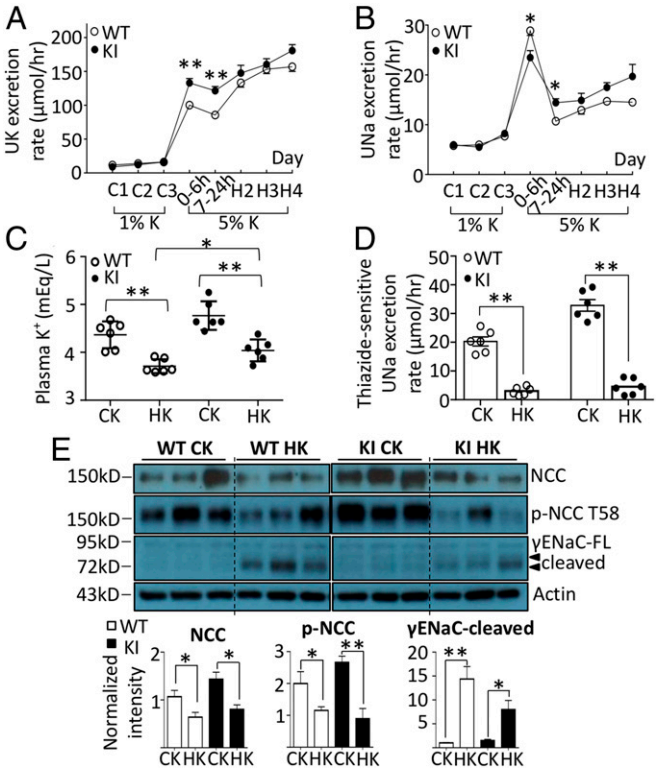

Fig. 4. Physiological and biochemical responses to long-term K^+ loading in WNK4 KI and WT mice. WT and WNK4 KI mice were fed a control K^+ (CK; 1% KCl) diet for 3 d (C1–C3) and then a K^+-rich diet (HK; 5% KCl) for 4 d (H1–H4). (*A* and *B*) The urinary K^+ (UK) and Na^+ (UNa) excretion rates in WT and KI mice taking HK were compared. (*C*) The plasma K^+ levels of mice at the end of 4 d on CK or HK diet were measured. (*D*) After a 4-d CK or HK diet, thiazide-sensitive UNa excretion rates in WT and KI mice were compared. (*E*) The protein abundance of total NCC and T58 phospho-NCC, and FL and cleaved forms of γENaC in WT and KI mice taking CK or HK diet ($n = 3$ for each group) were analyzed by Western blot. Mice in the same experiment were compared. The result shown is the representative of at least three experiments with similar results. Each band was quantified by ImageJ. $^*P < 0.05$; $^{**}P < 0.01$; NS, statistically not significant between indicated groups using Student's *t* test.

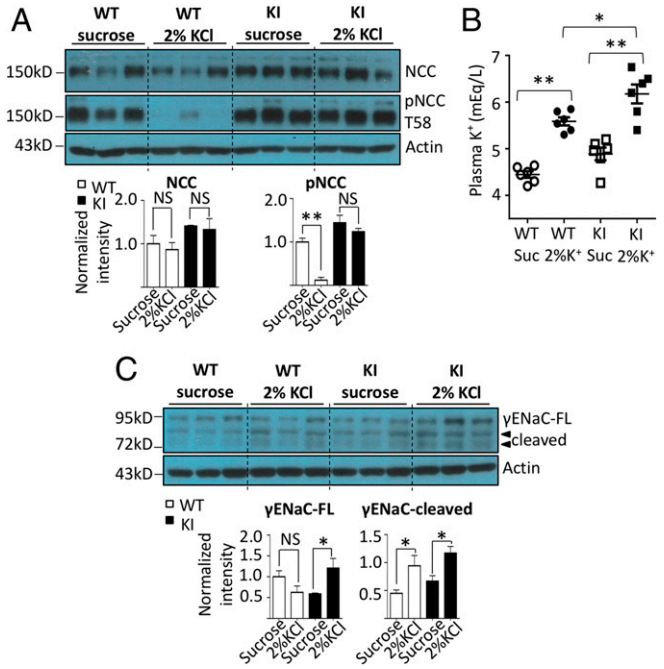

Fig. 5. Physiological and biochemical responses to acute K^+ loading in WNK4 KI and WT mice. WT and WNK4 KI mice received 2% sucrose solution (sucrose) or 2% sucrose solution containing 2% KCl (2%KCl) via gavage. The kidneys and blood were harvested at 30 min after gavage. (*A*) Total NCC and T58 phospho-NCC, (*C*) FL, and cleaved forms of γENaC in whole-kidney lysates of KI and WT mice taking sucrose or 2% KCl oral gavage ($n = 3$ for each group) were detected by Western blot. Mice in the same experiment were compared. The result shown is the representative of at least three experiments with similar results. (*B*) The plasma K^+ levels of mice were measured at 30 min after gavage.*$P < 0.05$; **$P < 0.01$; NS, statistically not significant between indicated groups, using Student's *t* test.

the turnover rate of NCC for NaCl, a small increase in driving force without appreciable decreases in $[Cl^-]_i$ may be sufficient to account for K^+-deficiency-induced enhancement of NaCl reabsorption in DCT. The process may be independent of WNK4. This argument is illustrated by the mechanism of water reabsorption in the proximal tubule. Reabsorption of NaCl in the proximal tubule is believed to generate an effective luminal hypotonicity to drive transtubular water reabsorption. The degree of luminal hypotonicity, however, is undetectable, thus yielding the term iso-osmotic water reabsorption in the proximal tubule.

To investigate the role of Cl^- sensing by WNK4 in vivo, we generated knockin mice carrying Cl^--insensitive L319F/L321F WNK4 mutant. We find that knockin mice phenotypically recapitulate human PHAII and mice carrying PHAII-mimicking gain-of-function WNK4 mutations. Thus, under baseline condition in DCT, the activity of WNK4 is inhibited by Cl^-, and loss of the inhibition results in increased activity. The results provide compelling support for the hypothesis that WNK4 is a physiological intracellular Cl^- sensor.

NCC-mediated Na^+ reabsorption in DCT controls Na^+ delivery to the downstream aldosterone-sensitive distal nephron, where Na^+ reabsorption via ENaC is important for K^+ secretion (22). Thus, NCC plays a critical role for K^+ homeostasis (14, 21). K^+ deficiency stimulates NCC to diminish Na^+ delivery to ENaC, curtailing K^+ secretion. Conversely, K^+ loading depresses NCC to enhance distal Na^+ delivery and K^+ excretion. Several studies have provided evidence to support the hypothesis that hypokalemia in K^+ deficiency lowers $[Cl^-]_i$ to activate WNK4 and NCC (10, 23, 24). Providing direct support for the hypothesis, we show that Cl^--insensitive WNK4 knockin mice with NCC hyperactivity are resistant to stimulation by K^+ deprivation, despite being responsive to other stimulation.

The mechanism of NCC inactivation by K^+ loading is less clear. Long-term K^+ loading decreases the abundance of total and phosphorylated NCC (27, 30, 31). Beyond that, it remains unsettled whether the WNK-SPAK/OSR1 kinase cascade or other additional mechanisms are involved. More recently, the role of protein phosphatases has been proposed (32–34). We find that 4 d of high-K^+ loading decreases NCC activity in knockin as well as WT mice. The results indicate that additional WNK4-independent mechanisms, such as activation of protein phosphatases, are involved (*SI Appendix*, Fig. S7). Although we cannot completely exclude the contribution of a WNK4 Cl^--sensing mechanism in our experiments, its contribution would be expected to be counterregulatory, given that our mice develop hypokalemia. In our experiments, hypokalemia on high-K^+ diets is likely a result of renal K^+ wasting from K^+ loading-induced natriuresis. In our search of published literature, we find that plasma $[K^+]$ in mice placed on chronic high-K^+ diets are variable (27, 30, 31). In one report, hypokalemia is also noted (35). Duration and composition of high-K^+ diets likely contribute to the variability of the findings.

In contrast to chronic high-K^+ loading, acute K^+ loading by either oral gavage or i.v. K^+ administration consistently causes hyperkalemia and NCC dephosphorylation within 15–30 min (21, 29, 36). In this study, we find that oral K^+ gavage increases plasma K^+ levels while decreasing the abundance of phospho-NCC in 30 min in WT mice. The decrease in phospho-NCC is not observed in knockin mice. This finding is consistent with the notion that high extracellular K^+ leads to elevation of $[Cl^-]_i$ and inhibits WNK4-mediated phosphorylation of NCC. To result in decreases in the abundance of phospho-NCC by turning off WNK4, NCC protein likely undergoes cycles of active phosphorylation and dephosphorylation at baseline. The hypothesis requires future investigation (see *SI Appendix*, Fig. S7 for the working model).

Three WNK kinases, WNK1, WNK3, and WNK4, are expressed in the kidney (1, 4). The role of WNK3 in the kidney is less clear, as *Wnk3*-knockout mice do not display renal phenotypes (37). The $[Cl^-]_i$ in DCT is reportedly 10–20 mM (20, 38). In vitro, the activity of WNK4 responds to 0–40 mM $[Cl^-]$, whereas the regulation of WNK1 and WNK3 kinase activity requires much higher $[Cl^-]$ (23). Consistent with the in vitro data, our study indicates that WNK4 is the main Cl^- sensor for regulation of NCC in mouse DCT under control K^+ diets. WNK1 is also expressed in DCT, and its overexpression leads to NCC activation (39). Future studies will investigate the role of WNK1 in DCT under different conditions, as well as its relationship with WNK4.

Methods

Animals. All experimental procedures for the mice study adhered to the guidelines of the Laboratory Animal Center and were approved by the Animal Care Committee of National Defense Medical Center. Cl^--insensitive L319F/L321F WNK4 knockin mice were generated using CRISPR/Cas9. For genotyping, mice tail clips were digested overnight in Viagen DirectPCR reagents with 0.2 mg/dL proteinase K at 56 °C and heat-inactivated by boiling in water bath for 5 min or at 85 °C for 45 min. Genomic DNA obtained from mice tail was used for genotyping PCR with the setting of hot start at 95 °C for 5 min, followed with 40 cycles at 95 °C for 30 s, 58 °C for 30 s, and 72 °C for 30 s, and ended with the extension step of 72 °C for 7 min. The forward and reverse primer sequences were 5′-CTGGAGTCGCCAGATTCTAC-3′ and 5′-CCCTAGATCAATAGCTCTGC-3′, respectively. The PCR products were digested by MscI overnight at 37 °C before electrophoresis.

Metabolic Cages and Diuretics Studies. Mice at 6–12 wk of age were used. The urine samples were collected by housing mice individually in a MMC100 metabolic cage (Hatteras Instruments). Blood samples were obtained via cheek pouch bleeding. To examine the response of mice to dietary K^+, mice were fed with a control K^+ diet (KCl 1%, TestDiet 5WGL) for 3 d, followed by 4 d of a high-K^+ diet (KCl 5%, TestDiet 9GT3) or a K^+-deficient diet (KCl <0.03%, TestDiet 9GT1). The 24-h urine samples were collected for 7 consecutive days. To study the acute response of mice, urine samples were

collected twice (0–6 and 7–24 h) on the first day of the high-K^+ or low-K^+ diet. The blood samples were obtained at the end of the 4-d dietary K^+ challenge. The urinary Na^+ and K^+ excretion rates were calculated by dividing total urinary Na^+ or K^+ excretion by the collecting time (μmol/h). In K^+ gavage experiments, mice received either 2% sucrose or 2% sucrose plus 2% KCl (512 nM) solution (15 μL/g body weight) (21). At 30 min after gavage, blood samples were collected for biochemistries, and kidneys were harvested for Western blot. In diuretic tests, mice were injected intraperitoneally with vehicle (0.9% NaCl with 2.5% DMSO) and then placed in metabolic cages to collect urine samples for 4 h. The next day, hydrochlorothiazide 12.5 mg/kg, furosemide 15 mg/kg, or amiloride 0.65 mg/kg was injected intraperitoneally, and the following 4-h urine sample was collected for analysis. The plasma and urine biochemistries were measured as described (40). The diuretic-sensitive urinary Na^+ excretion rate was defined by subtracting vehicle-induced urinary Na^+ excretion from diuretics-induced urinary Na^+ excretion. In these experiments, mice were always freely able to access to water. In norepinephrine test, norepinephrine (1,250 ng/g) or vehicle was injected peritoneally for 30 min before the mice were killed (28).

Blood Pressure Measurement. Systolic and diastolic blood pressures were measured with tail cuffs, using the Blood Pressure Analysis System (BP-98A; Softron). Mice were acclimated to the experimental procedure for 5 continuous days before the actual BPs were taken. The blood pressure of each mouse was taken 20 times every day, and the last 10 cycles of successfully measured BPs were taken for evaluation.

Western Blot Analysis. Kidneys were harvested from mice, total kidney extracts were obtained, and protein concentrations were measured as described (40). Total 20 μg lysates in Laemmli buffer were loaded onto an 8–10% SDS/PAGE gradient gel. After electrophoresis, separated proteins were transferred to nitrocellulose membrane (Amersham Protran 0.45 NC; GE) for Western blot analysis. The plasmid encoding full-length mouse WNK4 was a generous gift from M. Cobb (University of Texas Southwestern Medical Center). We raised the anti-NCC phospho-Thr-58 antibody against peptide F^{54}GYN (pT)IDVVP^{63} in rabbit and purchased the following antibodies: anti-WNK4 antibody (#5713; 1:1,000 dilution; Cell Signaling), anti-NCC antibody (AB3553; 1:5,000 dilution; Millipore), anti-NKCC2 (AB2281; 1:2,000 dilution; Millipore), anti-NKCC2 phospho-Ser-130 (S432C; 1:1,000 dilution; Dundee), anti-αENaC antibody (SPC-403D; 1:2,000 dilution; StressMarq), anti-βENaC antibody (1:1,000 dilution; StressMarq), anti-γENaC antibody (1:1,000 dilution; StressMarq), anti-SPAK (2281S; 1:500 dilution; Cell Signaling), anti-SPAK phospho-Ser-373 (S670B; 1:1,000 dilution; Dundee), anti-SPAK phospho-Ser-233 (S688B; 1:1,000 dilution; Dundee), anti-OSR1(S149C; 1:1,000 dilution; Dundee), and anti-ROMK (#APC-001; 1:1,000 dilution; Alomone laboratories). The secondary antibodies used in this study include anti-rabbit (1:4,000 dilution; Jackson Lab) and anti-sheep IgG antibody (1:10,000 dilution; Thermo Fisher Scientific). All the experiments were repeated at least three times, with similar results, and the data shown are from one representative experiment.

Data Analysis. Data analysis and curve fitting were performed with the Prism (v6.07) software (GraphPad Software). Data were presented as mean ± SEM. Statistical comparisons between two groups of data were made using a two-tailed unpaired Student's *t* test. Statistical significance was defined as *P* values less than 0.05.

ACKNOWLEDGMENTS. We thank the technical services provided by the Transgenic Mouse Model Core Facility of the National Core Facility Program for Biotechnology, Ministry of Science and Technology, Taiwan and the Gene Knockout Mouse Core Laboratory of National Taiwan University Center of Genomic Medicine. This study is supported by grants from Ministry of Science and Technology (MOST 106-2628-B-016-002-MY3, MOST 107-2314-B-016-010-MY3) and Tri-Service General Hospital (TSGH-C106-094 and TSGH-C107-095) in Taiwan. C.-L.H. is supported in part by grants from National Institutes of Health (DK111542).

1. Rodan AR, Jenny A (2017) WNK kinases in development and disease. *Curr Top Dev Biol* 123:1–47.
2. Cheng CJ, Rodan AR, Huang CL (2017) Emerging targets of diuretic therapy. *Clin Pharmacol Ther* 102:420–435.
3. McCormick JA, Ellison DH (2011) The WNKs: Atypical protein kinases with pleiotropic actions. *Physiol Rev* 91:177–219.
4. Dbouk HA, Huang CL, Cobb MH (2016) Hypertension: The missing WNKs. *Am J Physiol Renal Physiol* 311:F16–F27.
5. Boyden LM, et al. (2012) Mutations in kelch-like 3 and cullin 3 cause hypertension and electrolyte abnormalities. *Nature* 482:98–102.
6. Shibata S, Zhang J, Puthumana J, Stone KL, Lifton RP (2013) Kelch-like 3 and Cullin 3 regulate electrolyte homeostasis via ubiquitination and degradation of WNK4. *Proc Natl Acad Sci USA* 110:7838–7843.
7. Susa K, et al. (2014) Impaired degradation of WNK1 and WNK4 kinases causes PHAII in mutant KLHL3 knock-in mice. *Hum Mol Genet* 23:5052–5060.
8. Piala AT, et al. (2014) Chloride sensing by WNK1 involves inhibition of autophosphorylation. *Sci Signal* 7:ra41.
9. Bazúa-Valenti S, et al. (2015) The effect of WNK4 on the Na^+-Cl^- cotransporter is modulated by intracellular chloride. *J Am Soc Nephrol* 26:1781–1786.
10. Terker AS, et al. (2015) Potassium modulates electrolyte balance and blood pressure through effects on distal cell voltage and chloride. *Cell Metab* 21:39–50.
11. Lytle C, Forbush B, 3rd (1996) Regulatory phosphorylation of the secretory Na-K-Cl cotransporter: Modulation by cytoplasmic Cl. *Am J Physiol* 270:C437–C448.
12. Ponce-Coria J, et al. (2008) Regulation of NKCC2 by a chloride-sensing mechanism involving the WNK3 and SPAK kinases. *Proc Natl Acad Sci USA* 105:8458–8463.
13. Ohno M, et al. (2011) Immunolocalization of WNK4 in mouse kidney. *Histochem Cell Biol* 136:25–35.
14. Lalioti MD, et al. (2006) Wnk4 controls blood pressure and potassium homeostasis via regulation of mass and activity of the distal convoluted tubule. *Nat Genet* 38:1124–1132.
15. Wakabayashi M, et al. (2013) Impaired KLHL3-mediated ubiquitination of WNK4 causes human hypertension. *Cell Rep* 3:858–868.
16. Castañeda-Bueno M, et al. (2012) Activation of the renal Na^+:Cl^- cotransporter by angiotensin II is a WNK4-dependent process. *Proc Natl Acad Sci USA* 109:7929–7934.
17. Takahashi D, et al. (2014) WNK4 is the major WNK positively regulating NCC in the mouse kidney. *Biosci Rep* 34:e00107.
18. Yang YS, Xie J, Yang SS, Lin SH, Huang CL (2018) Differential roles of WNK4 in regulation of NCC *in vivo*. *Am J Physiol Renal Physiol* 314:F999–F1007.
19. Haas M, Forbush B, 3rd (2000) The Na-K-Cl cotransporter of secretory epithelia. *Annu Rev Physiol* 62:515–534.
20. Beck FX, Dörge A, Rick R, Schramm M, Thurau K (1987) Effect of potassium adaptation on the distribution of potassium, sodium and chloride across the apical membrane of renal tubular cells. *Pflugers Arch* 409:477–485.
21. Sorensen MV, et al. (2013) Rapid dephosphorylation of the renal sodium chloride cotransporter in response to oral potassium intake in mice. *Kidney Int* 83:811–824.
22. Rodan AR (2017) Potassium: Friend or foe? *Pediatr Nephrol* 32:1109–1121.
23. Terker AS, et al. (2016) Unique chloride-sensing properties of WNK4 permit the distal nephron to modulate potassium homeostasis. *Kidney Int* 89:127–134.
24. Penton D, et al. (2016) Extracellular K^+ rapidly controls NaCl cotransporter phosphorylation in the native distal convoluted tubule by Cl^- -dependent and independent mechanisms. *J Physiol* 594:6319–6331.
25. Rossier BC, Stutts MJ (2009) Activation of the epithelial sodium channel (ENaC) by serine proteases. *Annu Rev Physiol* 71:361–379.
26. Mente A, et al.; PURE Investigators (2014) Association of urinary sodium and potassium excretion with blood pressure. *N Engl J Med* 371:601–611.
27. Vallon V, Schroth J, Lang F, Kuhl D, Uchida S (2009) Expression and phosphorylation of the Na^+-Cl^- cotransporter NCC *in vivo* is regulated by dietary salt, potassium, and SGK1. *Am J Physiol Renal Physiol* 297:F704–F712.
28. Terker AS, et al. (2014) Sympathetic stimulation of thiazide-sensitive sodium chloride cotransport in the generation of salt-sensitive hypertension. *Hypertension* 64:178–184.
29. Rabinowitz L, Sarason RL, Yamauchi H (1985) Effects of KCl infusion on potassium excretion in sheep. *Am J Physiol* 249:F263–F271.
30. van der Lubbe N, et al. (2013) K^+-induced natriuresis is preserved during Na^+ depletion and accompanied by inhibition of the Na^+-Cl^- cotransporter. *Am J Physiol Renal Physiol* 305:F1177–F1188.
31. Castañeda-Bueno M, et al. (2014) Modulation of NCC activity by low and high K(+) intake: Insights into the signaling pathways involved. *Am J Physiol Renal Physiol* 306:F1507–F1519.
32. Hoorn EJ, et al. (2011) The calcineurin inhibitor tacrolimus activates the renal sodium chloride cotransporter to cause hypertension. *Nat Med* 17:1304–1309.
33. Picard N, et al. (2014) Protein phosphatase 1 inhibitor-1 deficiency reduces phosphorylation of renal NaCl cotransporter and causes arterial hypotension. *J Am Soc Nephrol* 25:511–522.
34. Shoda W, et al. (2017) Calcineurin inhibitors block sodium-chloride cotransporter dephosphorylation in response to high potassium intake. *Kidney Int* 91:402–411.
35. Murai I, Imanishi S, Sugimoto M, Kume S (2008) Effects of high potassium chloride supplementation on growth rate and renal function in mice. *Anim Sci J* 79:243–247.
36. Rengarajan S, et al. (2014) Increasing plasma [K^+] by intravenous potassium infusion reduces NCC phosphorylation and drives kaliuresis and natriuresis. *Am J Physiol Renal Physiol* 306:F1059–F1068.
37. Oi K, et al. (2012) A minor role of WNK3 in regulating phosphorylation of renal NKCC2 and NCC co-transporters *in vivo*. *Biol Open* 1:120–127.
38. Boettger T, et al. (2002) Deafness and renal tubular acidosis in mice lacking the K-Cl co-transporter Kcc4. *Nature* 416:874–878.
39. Vidal-Petiot E, et al. (2013) WNK1-related familial hyperkalemic hypertension results from an increased expression of L-WNK1 specifically in the distal nephron. *Proc Natl Acad Sci USA* 110:14366–14371.
40. Cheng CJ, Yoon J, Baum M, Huang CL (2015) STE20/SPS1-related proline/alanine-rich kinase (SPAK) is critical for sodium reabsorption in isolated, perfused thick ascending limb. *Am J Physiol Renal Physiol* 308:F437–F443.